



Moment of inertia for rock blocks subject to bookshelf faulting with geologically plausible density distributions

SOUMYAJIT MUKHERJEE

Department of Earth Sciences, Indian Institute of Technology Bombay, Powai, Mumbai 400 076, India.
e-mail: soumyajitm@gmail.com

MS received 13 July 2017; revised 29 November 2017; accepted 1 December 2017

Moment of Inertia (MOI) for rock blocks that glided smoothly into book-shelf dispositions are deduced considering realistic linear and exponential 3D variations in density along specific axes/directions. Knowing (empirical) algebraic relations of density with depth, which could also be anything other than the exponential and linear variations considered in this work, geoscientists can deduce the MOI by following the same process. MOI for a homogeneous parallelepiped block along any direction is proportional to the length of the block in that direction. However, this simple relation does not hold true for rock blocks with variable densities. Nevertheless, as the block length increases, the MOI along that direction would also increase.

Keywords. Rotational inertia; second moment of mass; density variation with depth; structural geology.

1. Introduction

Moment of Inertia (MOI), also known as ‘rotational inertia’ and ‘second moment of mass’ indicates distribution of mass in a body that tends to restrict its rotation, and expresses the ease or difficulty of that body to rotate. MOI is a well-established concept in statics (e.g., [Das and Mukherjee 2012](#)) and its expression for several regular geometric bodies has been deduced ([Spiegel and Liu 1999](#)). The MOI controls the state of rest or motion of a rotating body about its rotational axis. The greater the mass concentrated away from the axis of rotation, the greater the MOI. Thus, the MOI depends on the mass distribution inside a moving/deforming body ([Batra 2016](#)) that in turn is sensitive to any variations in density. Bykov ([2014, 2015](#)) used MOI in modeling seismicity related to rotation of fault blocks (also see [Dahlen 1977](#)). To be specific, Bykov ([2014, 2015](#)) presented a differential

equation involving inertial rotation angle, displacement and the MOI that represented the rotation waves in the ‘elastic fragmented massif’. [Dahlen \(1977\)](#), on the other hand, presented an expression of Earth in mechanical equilibrium during its rotation involving its MOI, and demonstrated mathematically how far this equilibrium disturbs locally due to faulting. Other applications of MOI can be found in engineering geology ([Hudson and Harrison 1992](#)), tectonics ([Bombolakis 1994](#)) and planetary sciences ([Margot et al. 2012](#)). For example, [Bombolakis \(1994\)](#) refined deformation behavior of rocks in modeled critical wedges that involved MOI in the analysis. Specifically, in structural geology, the MOI for fault blocks has been utilized in modeling the genesis of the related gouge material (equations 5 and 7 in [Guo and Morgan 2007](#); equations A2, A5 and A7 of [Guo and Morgan 2008](#)).

In case of book-shelf sliding, fault blocks rotate and slip by simple shear along pre-existing planes (figure 1), and are more common in deltaic shelf deposits (Mandl 1984, 1987, 2000), and also at times found in rift zones (Green *et al.* 2013). Such a deformation mechanism can work also on a microscopic scale amongst mineral grains (figure 2.23 in Mukherjee 2015). Tectonic loading is cited as one of the main factors for mega-scale bookshelf faulting (Narteau 2002). This work does not discuss ductile bookshelf sliding as recently discussed by Zuza and Yin (2013). Crustal blocks undergo rigid-body rotation so that the interfaces between individual blocks/books act as normal faults that rotate antithetically sheared with respect to the synthetic rotation (or primary simple shear) of the complete set of blocks/books. Deformations with these kinematics are of great importance in petroleum geosciences since the wide gaps that can develop along inter-block fault planes can transport hydrocarbons. Sediments deposited on the irregular top of bookshelf can form compaction synclines in which hydrocarbons can be stored preferentially in the hinge zone (Tin 1997). The bookshelf gliding of crustal blocks is important to seismicity studies (e.g., Wetzel *et al.* 1993), and has been elaborated using 2D Mohr diagrams and the Cosserat theory of elasticity

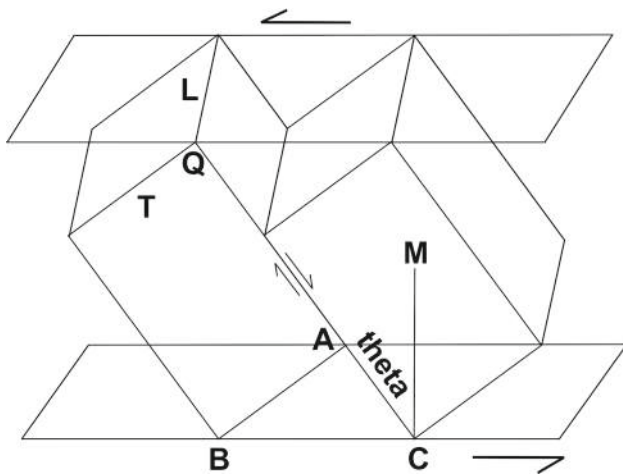


Figure 1. Top-to-left simple shear on crustal blocks/mineral grains produce book-shelf gliding. Antithetic top-to-right (down) shear between the two blocks. Compaction syncline produced at the top part of the slided blocks, in regional context. L: dimension of the block in the third perpendicular direction. T: thickness of the left block. CM: orientation of line CQ before shear. $\angle QCM = \theta$. In $\triangle ABC$, $AC = T \cdot \tan \theta$, Area $\triangle ABC = 0.5$, and $AB \cdot AC = 0.5 \cdot T^2 \cdot \tan \theta$. Volume of the space $V = 0.5 \cdot L \cdot T^2 \cdot \tan \theta$. By symmetry, the same volume is opened up at the top part as well.

(de Figueiredo *et al.* 2004). Also, Zuza and Yin (2016) deduced the velocity field along/across the displaced and rotated blocks in book-shelf faulting. Bookshelf gliding of mineral grains, often of micas and feldspars, are usually found in mylonites under an optical microscope (Meschede *et al.* 1997). The basal level of bookshelf normal faults can merge into a detachment (Peacock 1997). This article deduces MOI for bookshelf displaced and rotated blocks with geologically plausible density distributions.

Previous models of finding MOI involved constant density assumption for the faulted blocks. As stated in this work, in reality, density can vary either linearly or exponentially. Having considered that, the present work is an improved model of MOI for bookshelf glided blocks. Further, this work links the overall density of the rock with those of the pore fluid and the solid matrix, density gradients along different directions and the rock porosity. Finally, such an expression of density is linked with the MOI. With this model, therefore, one can test how MOI changes by changing its fundamental controlling factors. Testing the MOI in this way was not available in previous existing models.

2. Background and derivations

2.1 Case I

Density usually increases linearly vertically downward, especially for most oceanic crust (Reid 1987), sediments in basins (Motavalli-Anbaran *et al.* 2013), or even for the entire lithosphere (e.g., Xu *et al.* 2016) including the deep crust (Zhang and Chen 1992). However, the reverse can also happen (Ebbing *et al.* 2007 and its review) with depth, especially if evaporitic rocks are involved (Romer and Neugebauer 1991). An average density gradient can be $0.32 \text{ Mg m}^{-3} \text{ km}^{-1}$ (Carlson and Herrick 1990), or $13 \pm 2 \text{ kg m}^{-3} \text{ km}^{-1}$ (Tenzer *et al.* 2012). Metamorphism can induce gradual density gradients in any orientation in some cases (Zhou 2009). Sedimentary facies variation during marine to non-marine transitions would alter density progressively. Densities varying laterally in rocks can occur over distances of at least $\sim 20 \text{ km}$ (Wu and Mereu 1990).

Referring to figure 2, say at point $O(0, 0, 0)$ of a rectangular parallelepiped with dimensions x_1 , y_1 and z_1 along the axes X, Y and Z, the density is

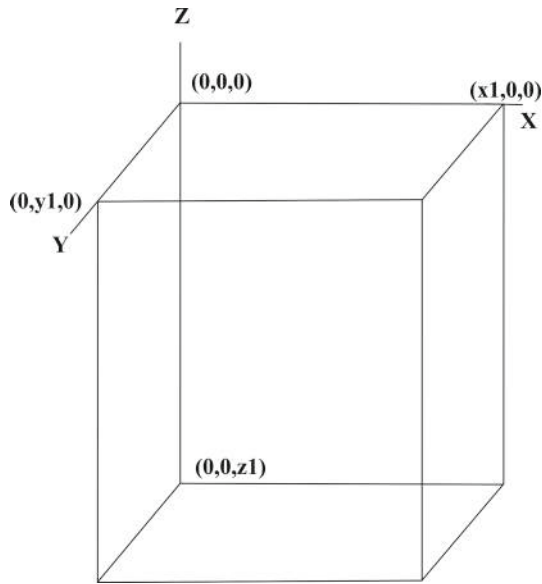


Figure 2. Co-ordinate system for the crustal block.

ρ_0 , and the linear density gradient in three perpendicular directions are k_i ($i = x, y, z$). Therefore, density variations along X-, Y- and Z-axes are:

$$\rho(x, 0, 0) = \rho_0 + k_x x, \quad (1)$$

$$\rho(0, y_0, 0) = \rho_0 + k_y y, \quad (2)$$

$$\rho(0, 0, z) = \rho_0 + k_z z. \quad (3)$$

Therefore, for any coordinate (x, y, z) , the density would be given by

$$\rho(x, y, z) = \rho_0 + k_x x + k_y y + k_z z. \quad (4)$$

The lateral variation of density (along X- and Y-directions) can be caused by excess pore fluid pressure in sediments (Buryakovsky *et al.* 1995). Note for $y = z = 0$, $x = y = 0$ and $z = x = 0$, equation (4) satisfies equations (1), (2) and (3), respectively. Secondly, obviously $k_x = k_y = k_z = 0$ would indicate a homogeneous block with constant density ' ρ_0 '. The MOI about the Y-axis is given by, as per Das and Mukherjee (2012)

$$I_y = \int_0^{x_1} \int_0^{y_1} \int_0^{z_1} \rho(x, y, z) (z^2 + x^2) dx dy dz. \quad (5)$$

Note that the volume of the block is

$$V = x_1 y_1 z_1. \quad (6)$$

The effective density of this block is

$$\rho_e = \{\rho_m - (\rho_m - \rho_f) \Phi_0\} + 0.5 \Sigma k_q q_1 \quad (7)$$

$(q = x, y, z)$ (Mukherjee 2017).

Putting $\rho(x, y, z)$ of equation (4) and 'V' of equation (6) into equation (5), integrating, and putting ρ_e of equation (10) in place of ρ_0 , and simplifying

$$I_y = 0.33 * V * \rho_e (z_1^2 + x_1^2) + k_x * x_1^2 (0.11 * z_1^2 + 0.25 * x_1) + 0.17 * k_y * y_1 (x_1^2 + z_1^2) + 0.5 * k_z z_1 (0.5 * z_1^2 + 0.33 * x_1^2). \quad (8)$$

2.2 Case II

2.2.1 Exponential variation of porosity with depth

An exponential depth-density relation can exist in sediments (Goteti *et al.* 2012), especially for argillaceous sediments presumably compacted to shallow depths (Rieke and Chilingarian 1974). These workers referred to the following relationship amongst bulk wet density of sediments (ρ_{bw}), matrix density (ρ_m), fluid density (ρ_f) and porosity (ϕ)

$$\rho_{bw} = \rho_m - (\rho_m - \rho_f) \phi. \quad (9)$$

On the other hand, Athy (1930) presented the following relation amongst surface porosity (ϕ_0), porosity at depth z (ϕ_z) and compaction constant $\lambda = b^{-1}$

$$\phi_z = \phi_0 e^{-bz}. \quad (10)$$

Combining equations (9 and 10),

$$\rho_{bwz} = \rho_m - (\rho_m - \rho_f) \phi_0 e^{-bz}. \quad (11)$$

Considering linear density variations along two horizontal perpendicular directions Y and Z as per equation (2) of Case I and equation (11), we get the following, in place of equation (4)

$$\rho(x, y, z) = \rho_m - (\rho_m - \rho_f) \phi_0 e^{-bz} + k_x x + k_y y. \quad (12)$$

Using equations (5 and 12)

$$I_y = V (z_1^2 + x_1^2) [0.33 * \rho_m + 0.5 * k_x * x_1 + 0.17 * k_y y_1] + (\rho_m - \rho_f) \phi_0 x_1 y_1 b^{-1} [0.33 * (e^{-bz_1} - 1) x_1^2 + e^{-bz_1} (z_1^2 + 2 * z_1 b^{-1} - 2 * b^{-2}) - 2 * b^{-2}]. \tag{13}$$

Recall, as per equation (6), here $V = x_1 y_1 z_1$. For $k_x = k_y = 0$, the expression simplifies to

$$I_y = V (z_1^2 + x_1^2) [0.33 * \rho_m] + (\rho_m - \rho_f) \phi_0 x_1 y_1 b^{-1} [0.33 * (e^{-bz_1} - 1) x_1^2 + e^{-bz_1} (z_1^2 + 2 * z_1 b^{-1} - 2 * b^{-2}) - 2 * b^{-2}]. \tag{14}$$

For the case of depth independent density, i.e.

$$b = 0 \tag{15}$$

or

$$\rho_{bwz} = \rho_m - (\rho_m - \rho_f) \phi_0. \tag{16}$$

One needs first to rewrite equation (4) as:

$$\rho(x, y, z) = \rho_m - (\rho_m - \rho_f) \phi_0 + k_x x + k_y y \tag{17}$$

and use that in equation (5) for integration.

2.2.2 Linear variation of porosity with depth

A deviation from a linear relation between density and depth is noted in overpressure zones (figure 2.7 of Telford *et al.* 1990). Unlike equation (10) in Case II, porosity can also decrease linearly with depth (Lerche and O'Brien 1987)

$$\emptyset_z = \emptyset_0 - cz \tag{18}$$

'c' is a constant. Therefore, equation (11) alters to

$$\rho_{bw} (0, 0, z) = \rho_{bwz} = \rho_m - (\rho_m - \rho_f) (\emptyset_0 - cz). \tag{19}$$

This linear relation between ρ_{bw} and z can also be expressed as equation (3) of Case I with $k_z = (\rho_m - \rho_f)$.

Note: (i) for constant magnitudes of $\rho_m, \rho_f, \Phi_0, x_1, z_1, k_i (i = x, y, z)$ in Case I and $k_i (i = x, y)$ in Case II, I_y is *not* proportional to y_1 . This is because I_y is either in the form of $I_y = Ay_1^2 + By_1$

or $I_y = Ay_1^2 + By_1 + C$. (ii) For the Case I, $k_i = 0$ would indicate a homogeneous block with spatially constant density = $\{\rho_m - (\rho_m - \rho_f)\Phi_0\}$. In that case

$$I_y = 0.33 * V \{\rho_m - (\rho_m - \rho_f) \Phi_0\} (z_1^2 + x_1^2) = 0.33 * M (z_1^2 + x_1^2) \tag{20}$$

where M is the mass of the block.

This matches with standard derivations available in statics texts for rectangular parallelepipeds. However, note that where we choose the Y-axis, whether inside, outside or at some other margin of the block, obviously modifies the expression for the MOI (derivations 11.2 in Spiegel and Liu 1999). Equation (20) for homogeneous block shows (recalling $V = x_1 y_1 z_1$), unlike the non-homogeneous case, $I_y \propto y_1$. This shows obviously that the presently considered MOI for the density-distributed blocks differ significantly from that of the homogeneous block case. Another point, if the density of the rock varies temporally, such as due to increased tectonic loading at its top, the present work would require a refinement in terms of time-dependent density.

2.2.3 Product of inertia

One can further deduce the product of inertia (POI) in the context of the tectonics and structural geology considered in this study. The POI has also been studied in the context of landscape pattern and geomorphological features (Zhang *et al.* 2006). In this case, the POI with respect to X- and Y-axes

$$I_{XY} = \int_0^{x_1} \int_0^{y_1} \rho(x, y, z) xy dx dy. \tag{21}$$

For Case I, substituting $\rho(x, y, z)$ from equation (4), and after performing definite integral

$$I_{XY} = 0.5 * x_1^2 y_1^2 [0.5(\rho_0 + k_x) + 0.33(k_x x_1 + k_y y_1)]. \tag{22}$$

Similarly,

$$I_{YZ} = 0.5 * y_1^2 z_1^2 [0.5(\rho_0 + k_x) + 0.33(k_x y_1 + k_y z_1)] \tag{23}$$

and

$$I_{ZX} = 0.5 * x_1^2 z_1^2 [0.5(\rho_0 + k_y) + 0.33(k_z y_1 + k_x z_1)]. \tag{24}$$

We firstly note that the POI increases *non-linearly* with increases in both the dimension of the parallelepiped (i.e., x_1 , y_1 and z_1) and its density gradient (k_i). Secondly, $I_{XY}, I_{YZ}, I_{ZX} \neq 0$. This means that neither of XY, YZ and XZ are the planes of symmetry, which as per figure 2 is obvious and matches our intuition. In other words, X-, Y- and Z-directions are not the principal axes at the corner point O. Thirdly, if we consider the X, Y and the Z axes passing through the point $(0.5x_1, 0.5y_1, 0.5z_1)$ and that this point is taken as the origin $(0, 0, 0)$, the POI becomes

$$I_{XY} = \int_{0.5x_1}^{0.5x_1} \int_{-0.5y_1}^{0.5y_1} \rho(x, y, z)xy \, dx \, dy$$

$$= I_{YZ} = I_{ZX} = 0. \quad (25)$$

This is for both the Cases I and II of $\rho(x, y, z)$ as per equations (4) and (12), respectively. This is as expected (Gere and Goodno 2009) since in this case the X-, Y- and Z-axes are the symmetry axes passing through the geometric centroid of the parallelepiped.

The following note can be made regarding equation (15) and later onwards in the main text that involves the following definite integral

$$\int_0^{z_1} (z^2 e^{-bz}) dz = b^{-1} [2 * b^{-2} - e^{-bz} (z_1^2 + 2 * z_1 b^{-1} + 2 * b^{-2})]. \quad (26)$$

One needs to consider the case of $b = 0$ before the definite integral operation, such as

$$\int_0^{z_1} z^2 \, dz = 0.33 * z_1^3. \quad (27)$$

Instead, if $b = 0$ is put on the right hand side of equation (26), the result is invalid since ‘ b ’ occurs also in the denominator.

3. Discussions

This article uses a few simple cases. In reality, both ρ_m and ρ_f can be depth (pressure and temperature) dependent (Djomani *et al.* 2001), while ρ_f can increase with depth (Patwardhan 2012). Even though the rock/sedimentary body remains ‘the same’ during bookshelf gliding, a change in ‘ ρ_f ’ that could be due to circulation of fluid along the fault plane would change the magnitude of MOI at any point inside the block. More refined

deductions of MOI can be attempted by optimists if required for tectonic modeling. In any case, we would require (at least empirical) equations (e.g., equations 1, 2 and 3 of Case I and equation 10 of Case II) of density variation within a rock/sediment column to find its MOI. Therefore, the present approach may not work as it is for book-shelf faulted blocks in metamorphic rocks, which are likely to have either locally non-specific (Reynolds 2011) or unknown density distributions (Gorbatsevich *et al.* 2017). Also note, since rotation rates that can only be constrained on faults >1 km long in tectonic/geological cases are very slow, e.g., 3° Ma^{-1} (Price and Scott 1994), $1-2^\circ \text{ Ma}^{-1}$ (Kreemer *et al.* 2009) or $0.25 \mu\text{rad yr}^{-1}$ (Sigmundsson 2006) with rotations of $\sim 22^\circ$ (Tapponnier *et al.* 1990) would take place over a long geological time with a total significant temporal change in ρ_f alone in the rotating block can alter the MOI.

Bookshelf gliding (figure 1) and rotational faulting are the two well known cases of deformation involving rigid body rotation in structural geology and tectonics. Of these two types of faults, the former affects rectangular parallelepiped crustal blocks *en mass*, so that analyzing their MOI for geologically realistic density distribution within blocks on scales of kms becomes relatively easy; it is much more difficult to constrain the slip rates of small scale bookcase faults. For faulted blocks with irregular geometric shapes, such as for rotationally faulted blocks (Mukherjee and Khonsari 2017), the analysis would become difficult. MOI of irregular objects can be deduced either experimentally (Koyama *et al.* 2010) or using computer models such as AMINERTIA (Internet reference).

4. Conclusions

The moment of inertia is deduced for book-shelf faulting of crustal blocks having geologically realistic density distributions. The deductions involve porosity, densities of rock matrix and that of the pore fluid. This work does not describe the evolution/genesis of such faulting, but estimates MOI when such a deformation takes place. Depending on their occurrence, such crustal blocks are potentially important in our understanding of ocean floor kinematics (Sigmundsson 2006), and in petroleum geosciences, their kinematic analyses become important, especially in analyzing basins formed above book-shelf faulted blocks (Veeken

2007; such as in the Afar region: Tapponnier *et al.* 1990). Considering the effect of porosity in the expression of MOI for bookshelf faulted blocks is important since such arrays are common in sedimentary environments, deltaic deposits in particular (Mandl 2000) where the density of each block is likely to be depth-controlled (along the Z-direction as per the present work). The MOI for the density-distributed blocks differ much from the case of the homogeneous block case, for example only for the latter case, the MOI about the Y-axis is proportional to the dimension of the parallelepiped along the Y-direction. The presented model is capable of handling MOI and POI for time-dependent density of the parallelepiped as well. The POI depends non-linearly on the length, width and height of the parallelepiped and its density gradient.

Acknowledgements

IIT Bombay provided a CPDA grant and a research sabbatical. Chhavi Jain (Yale University) supplied research papers. Thanks to Steven J Whitmeyer (James Madison University) and an anonymous reviewer for comments, and to Prof. Saibal Gupta (IIT Kharagpur) for handling and providing multiple rounds of comments in great detail. A special thanks to Chris Talbot (retired from Uppsala University) for improving my English. Vide Mukherjee (2017 and 2018a, b) and Mukherjee and Khonsari (submitted) for similar tectonic issues.

References

- Athy L F 1930 Density, porosity, and compaction of sedimentary rocks; *AAPG Bull.* **14** 1–22.
- Batra S 2016 *Physics: A Text Book for Class XI*; New Saraswati House India Pvt. Ltd., New Delhi.
- Bombolakis E G 1994 Applicability of critical-wedge theories to foreland belts; *Geology* **22** 535–538.
- Buryakovskiy L A, Djevanshir R Dj and Chilingar G V 1995 Abnormally-high formation pressures in Azerbaijan and the South Caspian Basin (as related to smectite – illite transformations during diagenesis and catagenesis); *J. Petrol. Sci. Eng.* **13** 203–218.
- Bykov V G 2015 Nonlinear waves and solutions in models of fault block geological media; *Russian Geol. Geophys.* **56** 793–803.
- Bykov V G 2014 Sine-Gordon equation and its application to tectonic stress transfer; *J. Seismol.* **18** 497–510.
- Carlson R L and Herrick C N 1990 Densities and porosities in the oceanic crust and their variations with depth and age; *J. Geophys. Res.* **95** 9153–9170.
- Dahlen F A 1977 The balance of energy in earthquake faulting; *Geophys. J. R. Astron. Soc.* **48** 239–261.
- Das B C and Mukherjee B N 2012 *Integral Calculus: Differential Equations*; 55th edn, U.N. Dhur & Sons Private Ltd., Kolkata, 574p.
- de Figueiredo R P, Vargas E do A Jr and Moraes A 2004 Analysis of bookshelf mechanisms using the mechanics of Cosserat generalized continua; *J. Struct. Geol.* **26** 1931–1943.
- Djomani Y H P, O'Reilly S Y, Griffin W L and Morgan P 2001 The density structure of subcontinental lithosphere through time; *Earth Planet. Sci. Lett.* **184** 605–621.
- Ebbing J, Braitenberg C and Wienecke S 2007 Insights into the lithospheric structure and tectonic setting of the Barents Sea region from isostatic considerations; *Geophys. J. Int.* **171** 1390–1403.
- Gere J M and Goodno B J 2009 *Mechanics of Materials*; 7th edn, Cengage Learning, 918p.
- Goteti G, Ings S J and Beaumont C 2012 Development of salt minibasins initiated by sedimentary topographic relief; *Earth Planet. Sci. Lett.* **339–340** 103–116.
- Green R G, White R S and Greenfield T S 2013 Bookshelf faulting and transform motion between rift segments of the Northern Volcanic Zone, Iceland; *Am. Geophys. Union Fall Meeting* 2013, Abstract #S51C–2381.
- Guo Y and Morgan J K 2007 Fault gouge evolution and its dependence on normal stress and rock strength – Results of discrete element simulations: Gouge zone properties; *J. Geophys. Res.* **112** B10403.
- Guo Y and Morgan J K 2008 Fault gouge evolution and its dependence on normal stress and rock strength—Results of discrete element simulations: Gouge zone Micromechanics; *J. Geophys. Res.* **113** B08417.
- Gorbatshevich F F, Kovalevskiy M V and Trishina O M 2017 Density and velocity model of metamorphic rock properties in the upper, middle and lower crust in the geospace of the Kola superdeep borehole (SG-3); *Geophys. Res. Abs.* **19** EGU2017–2155.
- Hudson J A and Harrison J P 1992 A new approach to studying complete rock engineering problems; *Quart. J. Eng. Geol.* **25** 93–105.
- <https://knowledge.autodesk.com/support/autocad-mechanical/learn-explore/caas/CloudHelp/cloudhelp/2015/ENU/AutoCAD-Mechanical/files/GUID-89D06668-A9CE-46D7-998B-AF61E00D1D5D-htm.html>
- Koyama Y M, Miranda H S, Cano A M and Barzellato B S S 2010 *Experimental determination of an irregular object's moment of inertia*; First International Congress on Instrumentation and Applied Sciences, Cancun Q.R. Mexico.
- Kreemer C, Blewitt G and Hammond W C 2009 Geodetic constraints on contemporary deformation in the Northern Walker Lane: 2. Velocity and strain rate tensor analysis; In: Late Cenozoic Structure and Evolution of the Great Basin – Sierra Nevada Transition (eds) Oldow J S and Cashman P H, *Geol. Soc. Am. Spec. Paper* **447** 17–31.
- Lerche I and O'Brien J J 1987 Modelling of buoyant salt diapirism; In: *Dynamical Geology of Salt and Related Structures* (eds) Lerche I and O'Brien J J, Academic Press, Orlando, pp. 129–162.
- Mandl G 1984 Rotating Parallel Faults; *AAPG Bull.* **68** 502–503.

- Mandl G 1987 Tectonic deformation of rotating parallel faults – the ‘bookshelf’ mechanism; *Tectonophysics*. **141** 277–316.
- Mandl G 2000 *Faulting in Brittle Rocks – An Introduction to the Mechanics of Tectonic Faults*; Springer-Verlag, Berlin, 274p.
- Margot J-L, Peale S J, Solomon S C, Hauck II S A, Ghigo F D, Jurgens R F, Yseboodt M, Giorgini J D, Padovan S and Campbell D B 2012 Mercury’s moment of inertia from spin and gravity data; *J. Geophys. Res.* **117** E00L09.
- Meschede M, Frisch W, Herrmann U R and Ratschbacher L 1997 Stress transmission across an active plate boundary: An example from southern Mexico; *Tectonophysics*. **266** 81–100.
- Motavalli-Anbaran S-H, Zeyen H and Ardestani V E 2013 3D joint inversion modeling of the lithospheric density structure based on gravity, geoid and topography data—application to the Alborz Mountains (Iran) and South Caspian Basin region; *Tectonophysics*. **586** 192–205.
- Mukherjee S 2015 *Atlas of Structural Geology*; Elsevier, Amsterdam, 60p.
- Mukherjee S 2017 Airy’s isostatic model: A proposal for a realistic case; *Arabian J. Geosci.* **10** 268, <https://doi.org/10.1007/s12517-017-3050-9>.
- Mukherjee S 2018a Locating center of pressure in 2D geological situations; *J. Ind. Geophys. Union* **22** 49–51.
- Mukherjee S 2018b Locating center of gravity in geological contexts; *Int. J. Earth Sci.* **107** 1935–1939.
- Mukherjee S and Khonsari M M 2018 Inter-book normal fault-related shear heating in brittle bookshelf faults; *Marine Petrol. Geol.* (**submitted**).
- Mukherjee S and Khonsari M M 2017 Brittle rotational faults and the associated shear heating; *Marine Petrol. Geol.* **88** 551–554, <https://doi.org/10.1016/j.marpetgeo.2017.09.003>.
- Narteau C 2002 Fault patterns under rotating conditions in a multiscale cellular automaton; *EGS General Assembly Conf. Abs.* **27**.
- Patwardhan A M 2012 *The dynamic Earth system*; 3rd edn, PHI Learning Pvt. Ltd., 491p.
- Peacock D C P 1997 Glossary of normal faults; *J. Struct. Geol.* **22** 291–305.
- Price S P and Scott B 1994 Fault block rotations at the edge of a zone of continental extension; southwest Turkey; *J. Struct. Geol.* **16** 381–392.
- Reid I 1987 Crustal structure of the Nova Scotian margin in the Laurentian Channel region; *Can. J. Earth Sci.* **24** 1859–1868.
- Reynolds J M 2011 *An Introduction to Applied and Environmental Geophysics*; Wiley-Blackwell.
- Rieke H H and Chilingarian C V 1974 *Compaction of argillaceous sediments*; Elsevier, Amsterdam, ISBN: 0-444-41054-6.
- Romer M-M and Neugebauer N J 1991 The salt dome problem: A multilayered approach; *J. Geophys. Res.* **96** 2389–2396.
- Sigmundsson F 2006 *Iceland Geodynamics: Crustal Deformation and Divergent Plate Tectonics*; Springer, Chichester, 141p.
- Spiegel M R and Liu J 1999 *Mathematical Handbook of Formulas and Tables*; 2nd edn, Schaum’s Outline Series, McGraw-Hill International Editions, New York, pp. 38–39.
- Tapponnier P, Armijo R, Manighetti I and Courtillot V 1990 Bookshelf faulting and horizontal block rotations between overlapping rifts in southern Afar; *Geophys. Res. Lett.* **17** 1–4.
- Telford W M, Geldart L P and Sheriff RE 1990 *Applied Geophysics*; 2nd edn, Cambridge University Press, New York, 17p, ISBN: 0-521-32693-1.
- Tenzer R, Baghebandi M and Vajda P 2012 Depth-dependent density change within the continental upper mantle; *Contrib. Geophys. Geodesy*, <https://doi.org/10.2478/v10126-012-001-z>.
- Tin N T 1997 Hydrocarbon trap styles of south eastern Vietnam offshore basins; *AAPG Database* 515–520 (http://archives.datapages.com/data/ipa/data/044/044001/515_ipa0440515.htm).
- Veeken P C H 2007 *Seismic Stratigraphy, Basin Analysis, and Reservoir Characterization*; Elsevier, Amsterdam, 318p.
- Wetzel L R, Wiens D A and Kleinrock M C 1993 Evidence from earthquakes for bookshelf faulting at large non-transform ridge offsets; *Nature* **362** 235–237.
- Wu J and Mereu R F 1990 The nature of the Kapuskasing structural zone: Results from the 1984 seismic refraction experiment; In: *Exposed cross-sections of the continental crust* (eds) Salisbury M H and Fountain D M, Kluwer Academic Publishers, pp. 563–586, ISBN: 13:978–94-010-6788-1.
- Xu Y, Zeyen H, Hao T, Santosh M, Li Z, Huang S and Xing J 2016 Lithospheric structure of the North China Craton: integrated gravity, geoid and topography data; *Gondwana Res.* **34** 315–323.
- Zhang C and Chen L 1992 Comprehensive study on stability of deep crust and unstable behavior of earthquake source by both failure mechanism and frictional sliding mechanism; *Acta Seismol. Sinica* **5** 503–514.
- Zhang S, Zhang J, Li F and Cropp R 2006 Vector Analysis theory on landscape pattern (VATLP); *Ecol. Mod.* **193** 492–502.
- Zhou Z 2009 3D vector gravity potential and line integrals for the gravity anomaly of a rectangular prism with 3D variable density contrast; *Geophysics* **74** 143–153.
- Zuza A V and Yin A 2013 Ductile bookshelf faulting: A new kinematic model for Cenozoic deformation in northern Tibet; AGU Fall Meeting Abstracts.
- Zuza A and Yin A 2016 Continental deformation accommodated by non-rigid passive bookshelf faulting: An example from the Cenozoic tectonic development of northern Tibet; *Tectonophysics*. **677–678** 227–240.